

Synthesis, Characterization, and Application of Antibody Functionalized Fluorescent Silica Nanoparticles

Matthew T. Hurley,* Zifan Wang, Amanda Mahle, Daniel Rabin, Qing Liu, Douglas S. English, Michael R. Zachariah, Daniel Stein, and Philip DeShong*

Fluorescent silica nanoparticles (FSNs) are prepared by incorporating dye into a mesoporous silica nanoparticle (MSN) synthesis procedure. FSNs containing sulforhodamine B, hydrophobically modified sulforhodamine B, and Cascade Blue hydrazide are made. The MSN-based FSNs do not leach dye under simulated physiological conditions and have strong, stable fluorescence. FSNs prepared with sulforhodamine B are compared to FSNs prepared with hydrophobically modified sulforhodamine B. The data indicate that FSNs prepared with sulforhodamine B are equally as stable but twice as fluorescent as particles made with hydrophobically modified sulforhodamine B. The fluorescence of a FSN prepared with sulforhodamine B is 10 times more intense than the fluorescence of a 4.5 nm core–shell CdSe/ZnS quantum dot. For diagnostic applications, a method to selectively and covalently bind antibodies to the surface of the FSNs is devised. FSNs that are functionalized with antibodies specific for *Neisseria gonorrhoeae* specifically bind to *Neisseria gonorrhoeae* in flow cytometry experiments, thus demonstrating the functionality of the attached antibodies and the potential of MSN-based FSNs to be used in diagnostic applications.

1. Introduction

Fluorescent silica nanoparticles (FSNs) have recently gained attention for their potential in diagnostic and detection applications. They have been used to image tumors,^[1] probe ligand-receptor interactions,^[2,3] and detect pathogens.^[3–6] They are particularly attractive for these applications because they can be prepared in a wide variety of colors, have strong stable fluorescence, and are biocompatible.^[7–12] Due to these

characteristics, FSNs have distinct advantages over quantum dot systems, which are used for similar applications. Quantum dots possess significant cytotoxicity and produce unstable fluorescence.^[13–15]

FSNs are typically prepared in one of two ways: (1) incorporation of siloxane-functionalized dyes into sol-gel silica nanoparticle synthesis^[4,6,11,13,16–27] (Figure 1, A); or (2) entrapment of dyes into silica nanoparticles prepared via microemulsion techniques^[5,7–10,12,28–35] (Figure 1B). In the first method, the siloxane-functionalized dye is hydrolyzed to a silicate derivative, undergoes polymerization with other silicate anions in solution, and becomes covalently incorporated into the silica framework of the nanoparticles. This methodology has also been employed to create mesoporous FSNs.^[36–39] In the second method (Figure 1B)^[40] silicate anions (from the hydrolysis of tetraethyl orthosilicate [TEOS]) and hydrophilic dye molecules reside within the aqueous phase of a water-oil microemulsion. As silicate polymerization occurs within the aqueous phase, the dye becomes entrapped within the Si-O-Si matrix, yielding FSNs.

Mesoporous silica nanoparticles (MSN) are synthesized by the templated polymerization of silicate around a surfactant mesophase.^[41,42] The surfactant within the as-synthesized MSN is then removed via calcination or chemical extraction, yielding mesoporous material. Figure 2 illustrates mobile crystalline material (MCM)-41 type MSN synthesis.^[41,42]

MSN are well known for their potential as controlled release and drug delivery systems. However, MSN-based fluorescent silica nanoparticles have been reported.^[43–50] Notably, Imai et al.^[45] and Sokolov et al.^[46–50] report making FSNs by incorporating dye molecules into MSN synthesis procedures. The authors concluded that dye is incorporated into the hydrophobic core of the surfactant micelles and becomes encased in the silica matrix (Figure 3).^[45,46] However, unlike standard MSN syntheses, the surfactant mesophases within the fluorescent silica particles are not removed via calcination or chemical extraction. This methodology provides an efficient, one-step synthesis of fluorescent silica nanoparticles. Yet, to the best of our knowledge, no one has used these MSN-based FSNs in diagnostic applications, such as flow cytometry or ELISA analysis.

Dr. M. T. Hurley, A. Mahle, D. Rabin, Dr. Q. Liu,
Dr. M. R. Zachariah, Dr. P. DeShong
Department of Chemistry and Biochemistry
University of Maryland
College Park, College Park, MD 20742, USA
E-mail: mhurley5@umd.edu; deshong@umd.edu

Z. Wang, Dr. D. S. English
Department of Chemistry
Wichita State University
Wichita, KS 67260, USA
Dr. D. Stein
Department of Cell Biology and Molecular Genetics
University of Maryland
College Park, College Park, MD 20742, USA

DOI: 10.1002/adfm.201202699



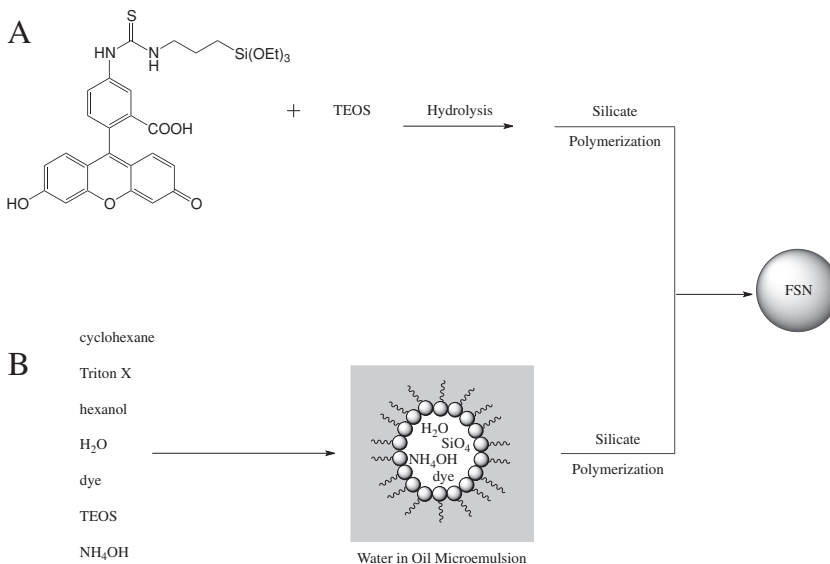


Figure 1. Common strategies used to prepare FSNs: A) Incorporation of siloxane-functionalized rhodamine into the sol-gel preparation of solid SiNPs. B) Incorporation of rhodamine into water in oil micro-emulsion techniques.

The use of the MSN-based FSNs in diagnostic applications is hindered by the fact that dye leaks from the FSNs because the dye molecules are non-covalently associated with the particles. Sokolov reported that rhodamine 6G diffused from their MSN-based fluorescent particles under aqueous conditions.^[46] To prepare MSN-based FSNs with optimum brightness that are suitable for in vitro and in vivo diagnostic applications, measures need to be taken to ensure that the encapsulated dye is retained within the silica nanoparticles.

Recently, Sokolov et al. reported that using alkylsiloxanes as silica co-precursors in their synthetic methodology yields FSNs that do not leach dye.^[48–50] The alkylsiloxane silica precursors incorporate hydrophobic groups into the silica matrix of the resulting particles. The authors hypothesize that the hydrophobic moieties inhibit dye diffusion by preventing water from entering the pores of the particles.^[48,49] However, the increased hydrophobicity of the particles may be problematic when developing the FSNs for use in diagnostic applications. To be used in flow cytometry or ELISA, the FSNs need to be functionalized with antibodies. However, proteins passively adsorb onto hydrophobically modified surfaces.^[51] Thus, due to the hydrophobic

nature of the particles, attached antibodies may passively adsorb onto the surface, denature, and lose their biological activity.

We proposed that adding hydrophobically modified dye into MSN synthesis would result in FSNs with increased dye incorporation due to the propensity of the modified dye to become incorporated into the surfactant mesophase, and moreover, the hydrophobically modified dye would be less likely to leach from the FSN due to increased hydrophobic interactions between the dye and surfactant mesophase. Thus, we anticipated that MSN-based FSNs prepared with hydrophobically modified dye would be brighter and more robust than MSN-based FSNs prepared using non-hydrophobically modified dye. Furthermore, by using hydrophobically modified dye, we expected that we would not need to alter the hydrophobicity of the silica matrix to prevent dye diffusion. Therefore, the goals of the research presented here were: (1) to characterize the fluorescent characteristics and stability of MSN-based FSNs

prepared using hydrophobically modified dye and MSN-based FSNs prepared using non-hydrophobically modified dye, and (2) to demonstrate that MSN-based FSNs can be functionalized with antibodies and then subsequently used to selectively bind and detect bacteria in flow cytometry.

2. Experimental Section

2.1. General

All chemicals were used as received from the supplier. 2-[methoxy(polyethyleneoxy)propyl]trimethoxysilane (PEGTMS) and (3-glycidoxypropyl)trimethoxysilane (GPTES) were purchased from Gelest, Inc. Tetraethyl orthosilicate (TEOS) and sulforhodamine B were purchased from Sigma-Aldrich. Pluronic F-127 was purchased from BASF. Cascade Blue hydrazide, trisodium salt, was purchased from Invitrogen. Fatty acid modified sulforhodamine B, 2, [1,2-dioleoyl-sn-glycero-3-phosphoethanolamine-N-(lissamine rhodamine B sulfonyl)] (ammonium salt) was purchased from Advanti Polar Lipids,

Inc. Core-shell CdSe/ZnS quantum dots stabilized with octadecylamine were purchased from Nanomaterials & Nanofabrication Laboratories. All aqueous solutions were made using water filtered through a Millipore water filtration system unless otherwise indicated. Phosphate buffered saline (PBS) solutions were prepared from phosphate buffered saline tablets obtained from Sigma-Aldrich (Sigma, tablets: P4417) as directed. The PBS solutions prepared had a measured pH of 7.4. An Ocean Optics USB 2000 spectrometer was used to obtain absorbance spectra. A Shimadzu RF-1501 spectrofluorophotometer

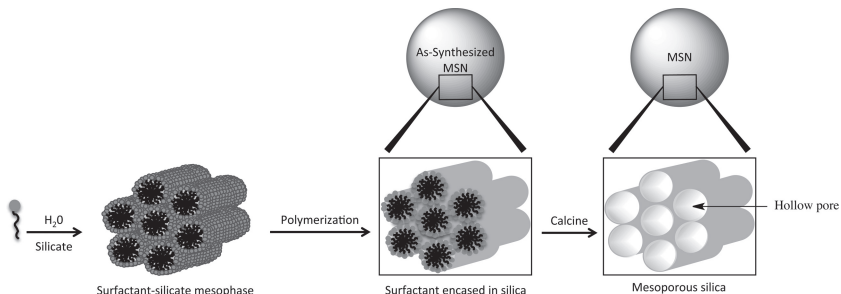


Figure 2. Schematic illustration of MCM-41 type mesoporous silica nanoparticle synthesis.^[42,43]

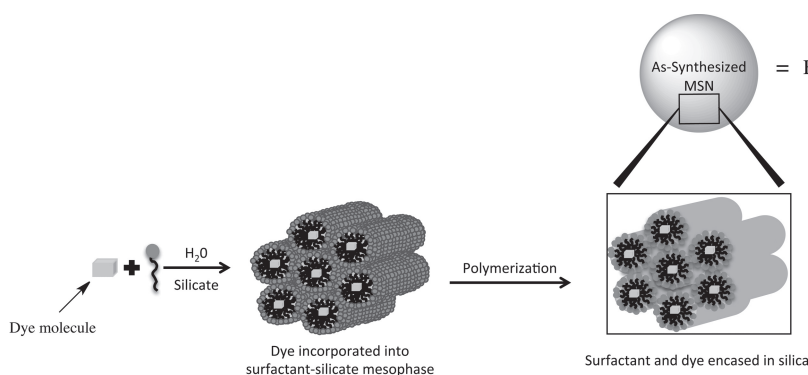


Figure 3. Schematic illustration of MSN-based fluorescent silica nanoparticle synthesis. Dye molecules are incorporated into the hydrophobic core of the surfactant mesophases, and then become entrapped within the silica matrix of the nanoparticles.

was used to obtain fluorescence spectra. Room temperature is defined as 20 °C.

2.2. MSN-Based Fluorescent Silica Nanoparticle Preparation

A standard procedure is as follows: fatty acid modified sulforhodamine B, 2, [1,2-dioleoyl-sn-glycero-3-phosphoethanolamine-N-(lissamine rhodamine B sulfonyl) (ammonium salt)] (0.001 g; 7.7×10^{-7} mol) was transferred to a three-necked round bottom flask in chloroform (1 mL) and dried in vacuo. Water (15 mL) and cetyltrimethylammonium bromide (CTAB) (0.050 g) were added to the reaction vessel followed by 3 mL of an aqueous solution containing lysine-HCl (0.017 g) and NaHCO₃ (0.012 g). The mixture was heated to 60 °C. To the vigorously stirring, heated reaction mixture was added a mixture of TEOS (0.532 mL) in heptane (5.00 mL). The TEOS/heptane mixture was added dropwise in ten 0.5 mL aliquots. The reaction mixture stirred at 60 °C for 2 h, giving rise to a red/pink precipitate. The reaction mixture was cooled and transferred to a centrifuge tube. The precipitate (FSN) was spun down and washed with PBS solution (10 mL) via centrifugation/resuspension three times and then dried in vacuo. Note: 0.44 mg (7.7×10^{-7} mol) of sulforhodamine B was used to prepared sulforhodamine B FSN.

2.3. Dye Release Studies

FSN (7.5 mg) were evenly suspended in PBS solution (4.00 mL) via sonication and then placed in a 25 °C water bath. A 2.0 mL aliquot was removed from the suspension and centrifuged. The absorbance of the supernatant was measured using an Ocean Optics USB 2000 spectrometer. The analyzed supernatant and the 2.0 mL aliquot were then returned to the sample suspension. This process was repeated every thirty minutes for three hours the first day. This process was repeated periodically over the next 7 days.

2.4. Fluorescence Imaging

Separate, dilute solutions of FSN and core-shell CdSe/ZnS quantum dots in toluene were spin-coated onto glass slides. The particles were excited with 514 nm wavelength light and the images were acquired using 0.11 μW laser power with 5 ms

dwell time per pixel. Integrated intensities, I_{ave} , were calculated using the equation:

$$I_{ave} = \frac{1}{N} \sum_i (I_i - B)$$

2.5. PEG Functionalized FSN

FSN (0.010 g) were suspended in toluene (5.00 mL) and sonicated until evenly dispersed. The solution was placed under an argon atmosphere. PEGTMS (0.610 mL, 1.3 mmol) was added to the rapidly stirring solution in one aliquot. The mixture stirred under argon atmosphere at room temperature for 2 h. The reaction mixture was transferred to a centrifuge tube. The functionalized particles were spun down and washed with toluene (5 mL) via centrifugation/resuspension three times and then dried in vacuo.

2.6. PEG/Epoxy Functionalized FSN

FSN (0.010 g) were suspended in toluene (5.00 mL) and sonicated until evenly dispersed. The solution was placed under an argon atmosphere. PEGTMS (0.610 mL, 1.3 mmol) was added to the rapidly stirring solution in one aliquot. The mixture stirred under argon atmosphere at room temperature for 30 minutes. An aliquot (0.100 mL) of a solution of GPTES (0.030 mL) in toluene (0.970 mL) (0.01 mmol of GPTES added) was then added to the reaction mixture. The mixture continued to stir under argon atmosphere at room temperature for 1.5 h. The reaction mixture was transferred to a centrifuge tube. The functionalized particles were spun down and washed with toluene (5 mL) via centrifugation/re-suspension three times and then dried in vacuo.

2.7. Conjugation of Goat Anti-Gonococcus IgG Antibody to PEG/Epoxy Functionalized FSN

PEG/Epoxy functionalized FSN (0.005 g) were suspended in PBS solution (1.50 mL). An aliquot (0.075 mL) of goat anti-gonococcus IgG antibody in PBS (2 mg/mL) was then added to the particle suspension. The reaction mixture was sonicated until particles were evenly dispersed, and then stirred at room temperature for 18 h. The particles were spun down and washed with PBS (5 mL) via centrifugation/re-suspension three times and then re-suspended in PBS (1 mL).

2.8. BCA Assay Protocol

BCA assays were conducted using reagents from a Pierce BCA Protein Assay Kit purchased from Thermo Scientific. The “enhanced test tube protocol” found in the instructions manual accompanying the BCA assay kit was employed. Briefly, an aliquot (0.100 mL) of a 5 mg/mL suspension of particles in PBS solution was transferred to a 1 dram vial. Freshly prepared BCA “working

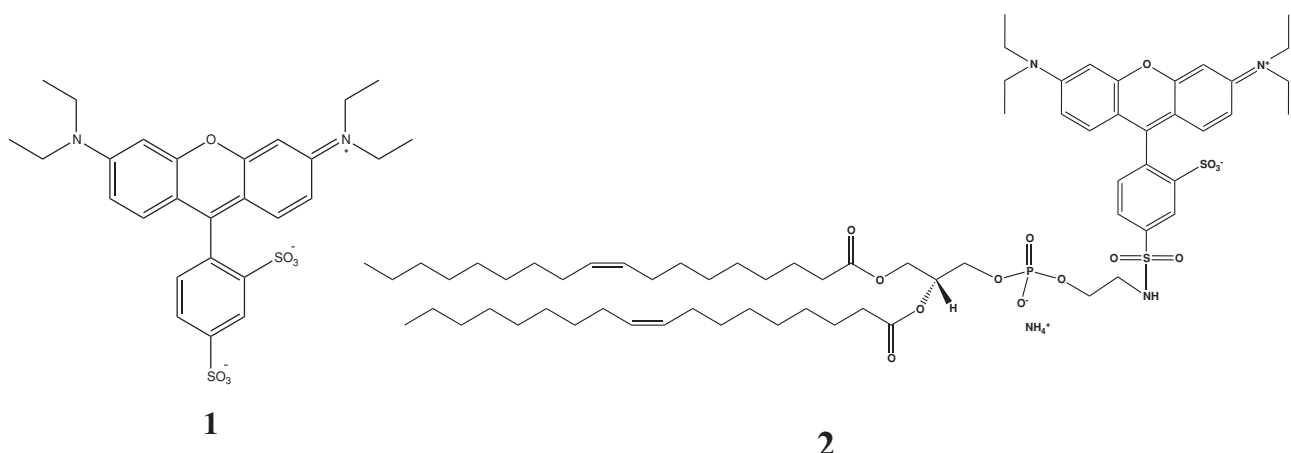


Figure 4. Structures of sulforhodamine B (1) and hydrophobically modified rhodamine B (2) used to prepare FSN.

reagent” (2.00 mL) was added to the vial. The vial was capped and placed in a water bath set at 60 °C for 30 min. Afterward, the vial was removed from the water bath and placed in a freezer for 10 min. The vial was removed from the freezer, allowed to warm to room temperature, and then the absorbance of the solution was measured using an Ocean Optics USB 2000 spectrometer.

2.9. Flow Cytometry

N. gonorrhoeae (GC) strain MS11Δopa was grown on gonococcal media base (GCK) agar plates, and *E. coli* on Luria Broth (LB) agar plates. The bacteria were grown for 20–24 h and resuspended in phosphate buffered saline (PBS) to an OD₆₅₀ of 0.8. Bacterial growth was halted by incubation of the cells with 100 µg/mL gentamicin sulfate for three hours at 37 °C. The suspensions were diluted to a concentration of 8 × 10⁵ cells/mL, incubated for 1 h with fluorescein isothiocyanate (FITC), and

then washed three times with PBS. The FITC-labeled bacteria were incubated with goat anti-gonococcus IgG functionalized Cascade Blue FSNs or polyethylene glycol (PEG) functionalized Cascade Blue FSNs for 1 hour at RT with moderate shaking, and then washed once with PBS. The cell suspensions were then subjected to FACS analysis using a FACSCanto II (BD Biosciences) flow cytometer. Data was analyzed with FACSDiva (BD Biosciences software).

3. Results and Discussion

3.1. MSN-Based FSN Synthesis

To compare particles prepared using hydrophobically modified dye with particles prepared using non-hydrophobically modified dye, two sets of particles were made—one with sulforhodamine B, 1, and one with fatty acid modified sulforhodamine B, 2 (Figure 4). The two sets of FSNs were prepared by introducing the dyes into the MSN synthesis protocol described by Okuyama.^[52] Okuyama's protocol was chosen because it yielded particles that were more monodispersed than particles prepared using other MSN synthetic strategies. The particles produced from this methodology were spherical with diameters of 90 ± 10 nm, and were highly fluorescent. Figure 5 depicts TEM images of the FSN produced by this method. The composition of the incorporated dye does not seem to affect the size or morphology of the FSN; particles prepared using the hydrophobically modified sulforhodamine B have the same diameter and morphology as particles prepared with sulforhodamine B.

3.2. Fluorescence Microscopy Analysis of FSN

The fluorescent properties of FSNs prepared using sulforhodamine B and the

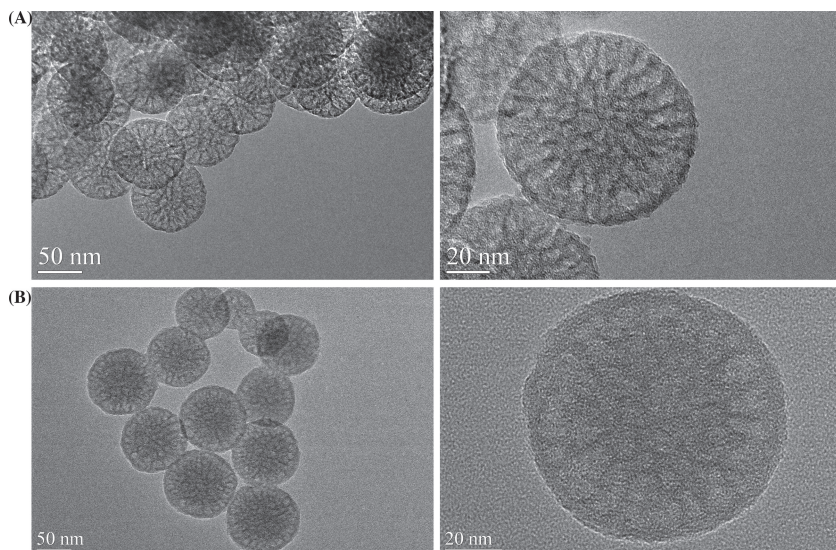


Figure 5. TEM images of prepared MSN-based FSN. A) FSN prepared using sulforhodamine B. B) FSN prepared using hydrophobically modified sulforhodamine B.

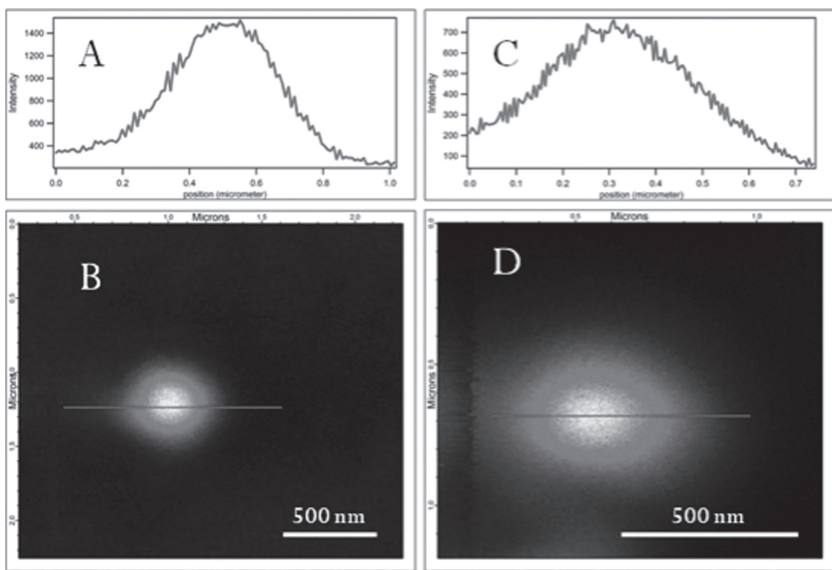


Figure 6. Comparison of fluorescence intensities of a FSN prepared with sulforhodamine B, 1 (panels A and B) and a FSN prepared using the hydrophobically modified sulforhodamine B, 2 (panels C and D). Panels A and B show the cross sectional intensity and fluorescence image, respectively, of an isolated FSN prepared using sulforhodamine B. Panels C and D show the cross sectional intensity and fluorescence image, respectively, of an isolated FSN prepared using hydrophobically modified sulforhodamine B.

hydrophobically modified counterpart were analyzed using confocal microscopy. **Figure 6** compares the fluorescence of a FSN prepared with hydrophobically modified sulforhodamine B with a FSN prepared using sulforhodamine B. It should be noted

that the two sets of FSNs that the samples in **Figure 6** were taken from were prepared with equal molar amounts of their respective dye. Though we anticipated that FSNs prepared with hydrophobically modified sulforhodamine B would be more fluorescent than FSNs prepared using sulforhodamine B, the FSN made with sulforhodamine B was twice as fluorescent as the particle made with the hydrophobically modified sulforhodamine B analogue. We attribute the preferential incorporation of the sulforhodamine B into the silica nanoparticle to electrostatic interactions between the cationic CTAB surfactant mesophase and the anionic sulforhodamine B molecules. Apparently, dyes which lack a hydrophobic tail can interact more effectively with the cationic charge and thus are incorporated preferentially.

The data presented in **Figure 7** compares the fluorescence intensity of a FSN prepared with sulforhodamine B to the fluorescence intensity of a 4.5 nm core–shell CdSe/ZnS quantum dot. The comparison to quantum dots is made because quantum dots have been used in similar fluorescence-based diagnostic applications as described below. While

we did not determine if the synthesis conditions employed yielded maximal incorporation of dye into the FSNs, we found that the FSN fluorescence was approximately 10 times brighter than that of the quantum dot. It is also noteworthy that the

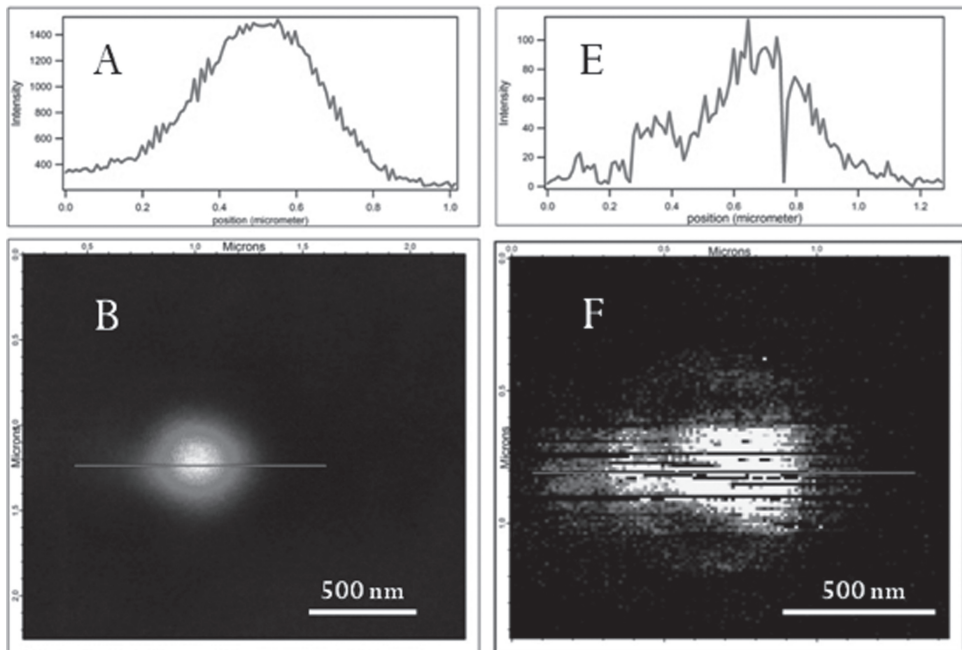


Figure 7. Comparison of fluorescence intensities of a FSN prepared using sulforhodamine B (panels A and B) and a 4.5 nm core–shell CdSe/ZnS quantum dot (panels E and F). Panels A and B show the cross sectional intensity and fluorescence image, respectively, of an isolated FSN prepared using sulforhodamine B. Panels E and F show the cross sectional intensity and fluorescence image, respectively, of an isolated 4.5 nm core–shell CdSe/ZnS quantum dot. Due to fluorescence intermittency, or blinking, the quantum dot appears as a series of streaks.

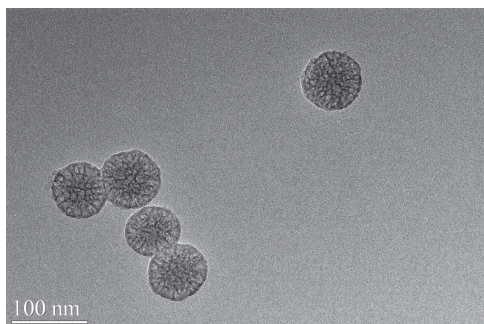


Figure 8. TEM image of Cascade Blue FSNs.

fluorescence of the FSN is more stable than the fluorescence of the quantum dot. Unlike the CdSe quantum dot, the FSN do not “blink”. As seen in Figure 7A,B, the FSN fluorescence signal is uniform and intense during the scanning process, while the CdSe quantum dot has a weaker fluorescence and less uniform fluorescence due to its propensity to undergo blinking. We anticipate that the strong, robust fluorescence from the FSN produced by this method will have many advantages over quantum dots in fluorescent assay technology.

To further demonstrate the fluorescent character of the MSN-based FSN, we also analyzed the fluorescence of a 100 nm FluoSphere obtained from Molecular Probes using confocal microscopy. The sulforhodamine B FSN has approximately the same fluorescent intensity as the FluoSphere (see the Supporting Information for data and experimental details).

3.3. Dye Retention by FSN

As mentioned above, for FSN to be suitable for in vitro and in vivo diagnostic applications, FSN cannot leach dye. To determine if dye leached from the prepared MSN-based FSNs under physiological conditions, FSNs prepared with sulforhodamine B and FSNs prepared with hydrophobically modified sulforhodamine B were separately suspended in PBS buffer at 25 °C and the supernatant was periodically analyzed using UV-vis spectroscopy (see the Experimental Section for details of the assay methodology). After standing in PBS solution at 25 °C for 7 days, no dye was detected in the supernatant for either FSN suspension (data not shown). These results indicate that neither set of FSNs release dye under simulated physiological conditions and both sets of particles would be suitable for diagnostic applications.

Considering the results reported by Sokolov et al.,^[46,50] it was surprising that no dye leached from the FSNs prepared with regular (non-hydrophobically modified) sulforhodamine B. Therefore, in order to determine if FSN stability was limited to sulforhodamine B, we repeated our synthesis, using a non-hydrophobically modified Cascade Blue dye (Cascade Blue hydrazide). Like the sulforhodamine B containing particles, the FSNs prepared with Cascade Blue hydrazide are approximately 90 nm in diameter (**Figure 8**), highly fluorescent, and do not leach dye after standing in PBS solution at 25 °C for 7 days.

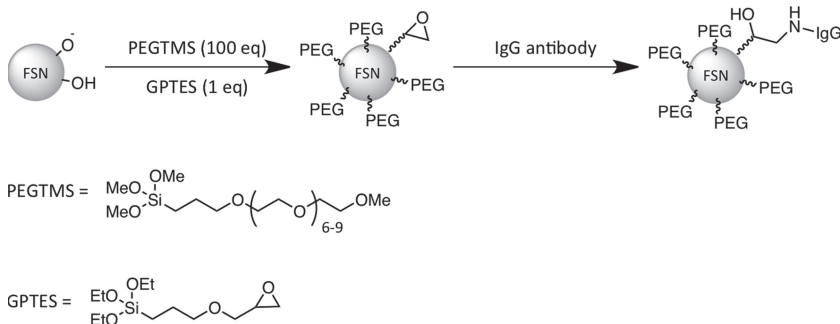
The discrepancy in the amount of dye released between Sokolov's FSNs and the FSNs described here may be attributed

to the different mesophase structures within the MSN-based FSNs. The different mesophase architectures are a result of the different synthetic methodologies used to prepare the MSN-based particles. In MSN formation, the structure of the surfactant-silicate mesophase is highly dependent on reaction mixture conditions, such as the concentration of the sol-gel components, pH, and temperature. Sokolov's method may result in particles with mesophases that are unable to retain dye as well as the mesophases within the FSNs prepared using our methodology. This hypothesis is supported by Sokolov's work where it is demonstrated that different release profiles are seen from MSN-based fluorescent particles containing different pore (mesophase) architectures.^[46] The difference in the surfactant to dye ratio in the sol-gel mixtures that were used to prepare the FSNs described in this report and the FSNs prepared by Sokolov could also explain why there is a difference in the amount of dye released between the two systems. Sokolov's sol-gel mixtures contain up to a 10:1 surfactant/dye molar ratio^[46–50] while our methodology uses a sol-gel mixture with an 80:1 surfactant/dye molar ratio. The increased surfactant to dye ratio in our FSNs would result in systems with increased hydrophobic interactions between the surfactant mesophases and dye molecules. Therefore, dye molecules are held more strongly within our particles and less dye is leached from our FSNs. We did not try to increase the amount of dye incorporated into our particles because we found that the fluorescence of the prepared FSNs was adequate for their intended diagnostic application described below.

The fact that highly water-soluble dyes, such as sulforhodamine B and Cascade Blue hydrazide, do not leach from our FSNs in aqueous media indicates that the dyes are tightly held within the surfactant mesophase. From this data, we expect that one should be able to make FSNs with a wide variety of dyes, and the FSNs would be stable and suitable for diagnostic applications. Recently, we have extended our methodology to create fluorescent porous silica nanoparticles that are similar to the systems described by Blanchard-Desce and coworkers.^[44,53]

3.4. Flow Cytometry Experiments

For application in flow cytometry, FSNs prepared with Cascade Blue hydrazide (Cascade Blue FSNs) were functionalized with antibody against the bacterial pathogen *Neisseria gonorrhoeae*. Antibody specific for gonococci was raised in a goat, and purified on a protein G column. Though several surface functionalization methodologies were attempted,^[54,55] it was found that immobilizing the antibody to FSN functionalized with a mixed polyethylene glycol (PEG)/epoxide coating was most effective in covalently conjugating the antibody to the particles and preventing the antibodies from passively absorbing^[56,57] and/or denaturing on the surface of the particles. Recently, Zhang^[58] and Chang^[59] successfully used similar strategies to bind antibodies to silica surfaces. **Scheme 1** depicts the functionalization strategy schematically. It is hypothesized that PEGTMS and GPTES form a mixed-multilayer on the silica surface as shown in **Figure 9**. Binding of antibody to FSN was verified using a standard bicinchoninic acid (BCA) colorimetric assay.^[60,61] An absorbance at 562 nm in the BCA assay indicates the presence



Scheme 1. Strategy used to prepare IgG-functionalized Cascade Blue FSNs.

of protein within the sample. The absorbance spectra from the BCA assay are shown in **Figure 10**. PEG/epoxide functionalized particles that were exposed to goat anti-gonococcus IgG antibody (referred to as IgG-functionalized FSNs in **Figure 10**) demonstrated an increased absorbance at 562 nm as compared to PEG/epoxide functionalized FSN that were not exposed to antibody—indicating that the antibody was successfully conjugated to the particles.

The ability of the anti-gonococcal IgG functionalized FSNs to bind to gonococci was analyzed by fluorescence-activated cell sorting (FACS). A series of control experiments were performed to demonstrate the fluorescent profiles of gonococci and various particle formulations. Gonococci were prelabeled with FITC to allow for their detection in the flow cytometer. The data indicate that the FITC-labeled gonococci were all detected in quadrant 4, demonstrating strong fluorescence at 588 nm (**Figure 11A**). The data in **Figure 11B** shows the fluorescence profile of bare, non-functionalized Cascade Blue FSNs. The presence of a small population in Q3 indicates that in the initial synthesis, a small population of particles was made that poorly incorporated dye into the particle. The fluorescent profiles of PEG

functionalized Cascade Blue FSNs and anti-gonococcal IgG functionalized Cascade Blue FSNs are depicted in **Figure 11C,D**, respectively. The average fluorescence of the particles did not decrease after functionalization, indicating that no dye leached from the particles during the functionalization procedures.

Gonococci were mixed with anti-gonococcal IgG functionalized Cascade Blue FSNs, washed and the resulting population of gonococci analyzed by FACS (**Figure 11E**). The double-positive population in quadrant 2 demonstrates that the IgG-functionalized Cascade Blue FSN recognize and bind to the FITC-labeled *N. gonorrhoeae*.

To demonstrate the specificity of binding of the anti-gonococcal IgG functionalized Cascade Blue FSNs, FITC-labeled gonococci were mixed with PEG functionalized Cascade Blue FSNs, washed, and then subjected to FACS. The data in **Figure 11 F** demonstrate the lack of binding to gonococci by the PEG coated particles. Furthermore, when anti-gonococcal IgG functionalized Cascade Blue FSNs were mixed with FITC-labeled *Escherichia coli*, a single population is present, representing FITC-labeled *E. coli* (**Figure 11G**). This data indicates that the anti-gonococcal IgG functionalized FSNs do not bind to *E. coli*.

Taken together, the FACS data demonstrate that the anti-gonococcal IgG functionalized FSNs selectively bind to *N. gonorrhoeae*. Moreover, the results indicate that the IgG antibodies attached to the surface of the FSNs are functional and that IgG functionalized MSN-based FSNs can be used as diagnostic tools.

We noted a decrease in fluorescence intensity of the Cascade Blue FSN associated with the FITC-labeled GC, and hypothesized that FITC was quenching the fluorescence of Cascade Blue. We measured the effect of FITC on Cascade Blue fluorescence by mixing various concentrations of FITC with Cascade Blue hydrazide. As shown in **Figure 12**, the fluorescence intensity of Cascade Blue hydrazide decreases with increasing FITC concentration, thus demonstrating that Cascade Blue hydrazide fluorescence is quenched by FITC.

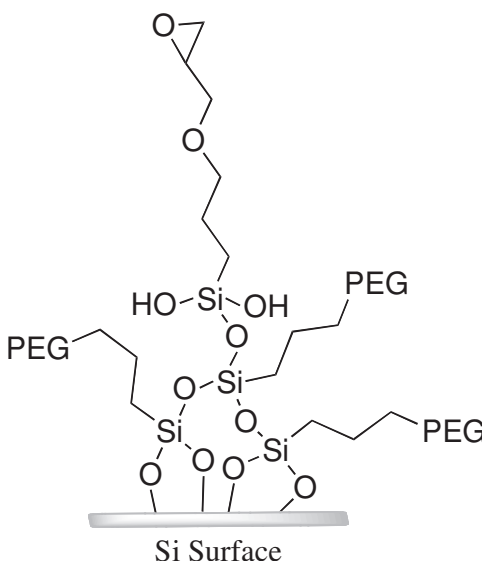


Figure 9. Proposed mixed-multilayer formed on PEGTMS/GPTES functionalized FSNs.

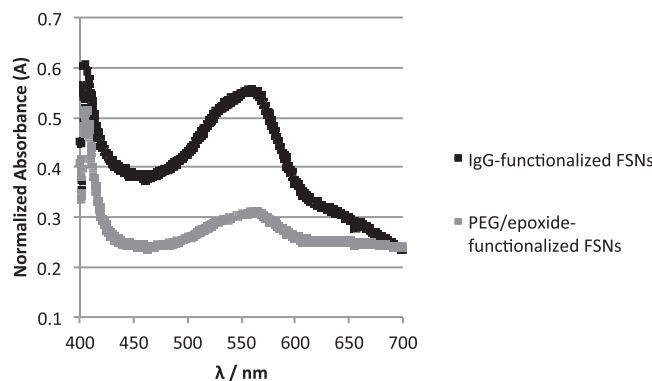


Figure 10. Absorbance spectra from the BCA assay of goat anti-gonococcus IgG antibody functionalized FSNs (black) and PEG/epoxide functionalized FSNs (grey; control). Absorbance at 560 nm indicates the presence of protein within the sample. The slight positive result seen for PEG/epoxide-functionalized FSNs is attributed to chemical interference with the assay.

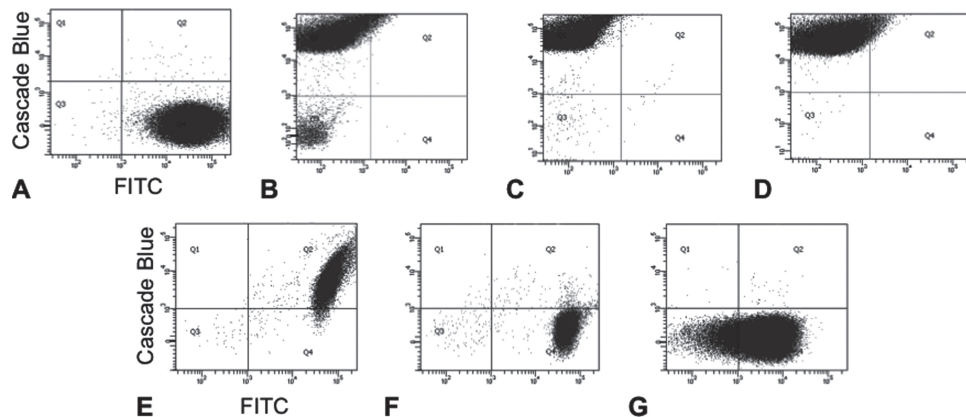


Figure 11. Flow cytometry using anti-gonococcal IgG functionalized FSNs. A) FITC labeled Gonococci. B) Non-functionalized Cascade Blue FSNs. C) PEG functionalized Cascade Blue FSNs. D) Anti-gonococcal IgG functionalized Cascade Blue FSNs. E) Anti-gonococcal IgG functionalized Cascade Blue FSNs with FITC labeled *E. coli*. F) PEG functionalized Cascade Blue FSNs with FITC labeled Gonococci. G) Anti-gonococcal IgG functionalized Cascade Blue FSNs with FITC labeled *E. coli*. The voltage of the photomultiplier tube (PMT) utilized for the particles alone was 445, and for the particles with bacteria it was 588. This discrepancy in detector voltage was due to the observed quenching of cascade blue by FITC. The profiles were gated on aggregates, eliminating cellular debris and background noise. Panel G was gated on all events due to a lack of *E. coli* aggregation.

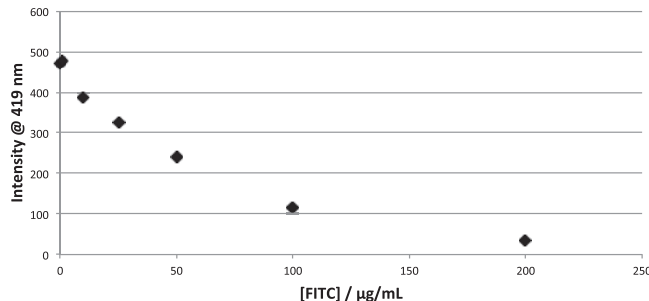


Figure 12. Quenching of Cascade Blue fluorescence by FITC. Data points were obtained by measuring the fluorescence of Cascade Blue hydrazide solutions containing varying amounts of FITC. The concentration of Cascade Blue hydrazide in each solution was 1 $\mu\text{g}/\text{mL}$. Solutions were prepared using PBS. Cascade Blue hydrazide fluorescence intensity was measured at 419 nm. The excitation wavelength used was 380 nm.

4. Conclusions

FSNs were prepared by incorporating dye into a mesoporous silica nanoparticle synthesis procedure. FSNs prepared using sulforhodamine B were two-times more fluorescent than particles made with the hydrophobically modified sulforhodamine B analogue. The FSNs produced by this method do not leach dye under physiological conditions and have strong, stable fluorescence. A FSN prepared using sulforhodamine B was ~10 times more fluorescent than a 4.5 nm core-shell CdSe/ZnS quantum dot.

Antibody functionalized Cascade Blue FSNs were prepared for use in flow cytometry, and the results from flow cytometry demonstrate that anti-gonococcus IgG functionalized FSN selectively bind to *N. gonorrhoeae* and have the ability to be used in diagnostic applications.

Supporting Information

Supporting Information is available from the Wiley Online Library or from the author.

Acknowledgements

P.D. and M.Z. acknowledge the generous financial support of the National Science Foundation (NIRT, CHE 0511219478, "Stimuli-Response Hybrid Nanoparticles for Controlled Chemical Delivery"), the Maryland Technology Development Corporation, and SD Nanosciences, Inc. We gratefully acknowledge the support of the Maryland NanoCenter and its NispLab. The NispLab is supported in part by the NSF as a MRSEC Shared Experimental Facility. M.T.H. acknowledges the support of the Graduate Assistance in Areas of National Need (GAANN) Fellowship. D.C.S. acknowledges the support from a grant from the National Institutes of Health (AI068888). A.M. was supported by a T32 training grant from the National Institutes of Health (AI09621).

Received: September 17, 2012

Revised: November 28, 2012

Published online: February 11, 2013

- [1] J. Wan, X. Meng, E. Liu, K. Chen, *Nanotechnology* **2010**, *21*, 235104.
- [2] L.-Z. Yang, Z.-L. Chen, *Anal. Lett.* **2011**, *44*, 687–697.
- [3] X. Wang, O. Ramstrom, M. Yan, *Chem. Commun.* **2011**, *47*, 4261–4263.
- [4] D. Qin, X. He, K. Wang, W. Tan, *Biosens. Bioelectron.* **2008**, *24*, 626–631.
- [5] Z. Wang, T. Miu, H. Xu, N. Duan, X. Ding, S. Li, *J. Microbiol. Methods* **2010**, *83*, 179–184.
- [6] X. Zhang, C. Song, L. Chen, K. Zhang, A. Fu, B. Jin, Z. Zhang, K. Yang, *Biosens. Bioelectron.* **2011**, *26*, 3958–3961.
- [7] K. Fent, C. J. Weisbrod, A. Wirth-Heller, U. Pieles, *Aquat. Toxicol.* **2010**, *100*, 218–228.
- [8] H. Ow, D. R. Larson, M. Srivastava, B. A. Baird, W. W. Webb, U. Wiesner, *Nano Lett.* **2005**, *5*, 113–117.
- [9] I. Sokolov, S. Naik, *Small* **2008**, *4*, 934–939.
- [10] S.-W. Ha, C. E. Camalier, G. R. Beck, Jr., J.-K. Lee, *Chem. Commun.* **2009**, 2881–2883.
- [11] E. Herz, T. Marchincin, L. Connelly, D. Bonner, A. Burns, S. Switalski, U. Wiesner, *J. Fluoresc.* **2010**, *20*, 67–72.

- [12] S. Roy, R. Woolley, B. D. MacCraith, C. McDonagh, *Langmuir* **2010**, *26*, 13741–13746.
- [13] S. G. Penn, L. He, M. J. Natan, *Curr. Opin. Chem. Biol.* **2003**, *7*, 609–615.
- [14] E. Katz, I. Willner, *Angew. Chem., Int. Ed.* **2004**, *43*, 6042–6108.
- [15] Zhong Wenwan, *Anal. Bioanal. Chem.* **2009**, *394*, 47–59.
- [16] H. Langhals, A. J. Esterbauer, *Chem. Eur. J.* **2009**, *15*, 4793–4796.
- [17] M. Faisal, Y. Hong, J. Liu, Y. Yu, J. W. Y. Lam, A. Qin, P. Lu, B. Z. Tang, *Chem. Eur. J.* **2010**, *16*, 4266–4272.
- [18] C. Xie, D. Yin, J. Li, L. Zhang, B. Liu, M. Wu, *Nano Biomed. Eng.* **2009**, *1*, 39–47.
- [19] A. Burns, P. Sengupta, T. Zedayko, B. Baird, U. Wiesner, *Small* **2006**, *2*, 723–726.
- [20] N. A. M. Verhaegh, A. V. Blaaderen, *Langmuir* **1994**, *10*, 1427–1438.
- [21] M. Montalti, L. Prodi, N. Zaccheroni, A. Zattoni, P. Reschiglian, G. Falini *Langmuir* **2004**, *20*, 2989–2991.
- [22] X.-L. Chen, J.-L. Zou, T.-T. Zhao, Z.-B. Li, *J. Fluoresc.* **2007**, *17*, 235–241.
- [23] J. Folling, S. Polyakova, V. Belov, A. van Blaaderen, L. Bossi Mariano, W. Hell Stefan, *Small* **2008**, *4*, 134–142.
- [24] A. J. Moro, J. Schmidt, T. Doussineau, A. Lapresta-Fernandez, J. Wegener, G. J. Mohr, *Chem. Commun.* **2011**, *47*, 6066–6068.
- [25] Y.-S. Cho, T.-J. Yoon, E.-S. Jang, K. Soo Hong, S. Young Lee, O. Ran Kim, C. Park, Y.-J. Kim, G.-C. Yi, K. Chang, *Cancer Lett.* **2010**, *299*, 63–71.
- [26] Y. Wang, J. C. Gildersleeve, A. Basu, M. B. Zimmt, *J. Phys. Chem. B* **2010**, *114*, 14487–14494.
- [27] H. Langhals, A. J. Esterbauer, *Chem. Eur. J.* **2009**, *15*, 4793–4796.
- [28] X. Gao, J. He, L. Deng, H. Cao, *Opt. Mater.* **2009**, *31*, 1715–1719.
- [29] H.-H. Yang, H.-Y. Qu, P. Lin, S.-H. Li, M.-T. Ding, J.-G. Xu, *Analyst* **2003**, *128*, 462–466.
- [30] S. Santra, P. Zhang, K. Wang, R. Tapec, W. Tan, *Anal. Chem.* **2001**, *73*, 4988–4993.
- [31] J. Godoy-Navajas, M.-P. Aguilar-Caballos, A. Gomez-Hens, *J. Fluoresc.* **2010**, *20*, 171–180.
- [32] K. S. Yao, S. J. Li, K. C. Tzeng, T. C. Cheng, C. Y. Chang, C. Y. Chiu, C. Y. Liao, J. J. Hsu, Z. P. Lin, *Adv. Mater. Res.* **2009**, *513*–516.
- [33] A. Cao, Z. Ye, Z. Cai, E. Dong, X. Yang, G. Liu, X. Deng, Y. Wang, S.-T. Yang, H. Wang, M. Wu, Y. Liu, *Angew. Chem., Int. Ed.* **2010**, *49*, 3022–3025.
- [34] K. G. Lee, J. C. Kim, R. Wi, J. S. Min, J. K. Ahn, D. H. Kim, *J. Nanosci. Nanotechnol.* **2011**, *11*, 686–690.
- [35] K. G. Lee, R. Wi, T. J. Park, S. H. Yoon, J. Lee, S. J. Lee, D. H. Kim, *Chem. Commun.* **2010**, *46*, 6374–6376.
- [36] C. E. Fowler, S. Mann, B. Lebeau, *Chem. Commun.* **1998**, 1825–1826.
- [37] B. Lebeau, C. E. Fowler, S. Mann, C. Faracet, B. Charleux, C. Sanchez, *J. Mater. Chem.* **2000**, *10*, 2105–2108.
- [38] Y.-S. Lin, C.-P. Tsai, H.-Y. Huang, C.-T. Kuo, Y. Hung, D.-M. Huang, Y.-C. Chen, C.-Y. Mou, *Chem. Mater.* **2005**, *17*, 4570–4573.
- [39] I. Slowing, B. G. Trewyn, V. S. Y. Lin, *J. Am. Chem. Soc.* **2006**, *128*, 14792–14793.
- [40] V. Chhabra, V. Pillai, B. K. Mishra, A. Morrone, D. O. Shah, *Langmuir* **1995**, *11*, 3307–3311.
- [41] C. T. Kresge, M. E. Leonowicz, W. J. Roth, J. C. Vartuli, J. S. Beck, *Nature* **1992**, *359*, 710–712.
- [42] A. Firouzi, F. Atef, A. G. Oertli, G. D. Stucky, B. F. Chmelka, *J. Am. Chem. Soc.* **1997**, *119*, 3596–3610.
- [43] L. A. Rocha, J. M. A. Caiut, Y. Messaddeq, S. J. L. Ribeiro, M. A. U. Martines, J. d. C. Freiria, J. Dexpert-Ghys, M. Verelst, *Nanotechnology* **2010**, *21*, 155603.
- [44] V. Lebret, L. Raehm, J.-O. Durand, M. Smaihi, C. Gerardin, N. Nerambourg, M. H. V. Werts, M. Blanchard-Desce, *Chem. Mater.* **2008**, *20*, 2174–2183.
- [45] S. Muto, Y. Oaki, H. Imai, *Chem. Lett.* **2006**, *35*, 880–881.
- [46] I. Sokolov, Y. Y. Kievsky, J. M. Kaszpurenko, *Small* **2007**, *3*, 419–423.
- [47] I. Sokolov, S. Naik, *Small* **2008**, *4*, 934–939.
- [48] E.-B. Cho, D. O. Volkov, I. Sokolov, *Small* **2010**, *6*, 2314–2319.
- [49] E.-B. Cho, D. O. Volkov, I. Sokolov, *Adv. Funct. Mater.* **2011**, *21*, 3129–3135.
- [50] D. O. Volkov, E.-B. Cho, I. Sokolov, *Nanoscale* **2011**, *3*, 2036–2043.
- [51] Z.-J. Zhu, T. Posati, F. Moyano Daniel, R. Tang, B. Yan, W. Vachet Richard, M. Rotello Vincent, *Small* **2012**, DOI: 10.1002/smll.201200794.
- [52] A. B. D. Nandiyanto, S. G. Kim, F. Iskandar, K. Okuyama, *Microporous Mesoporous Mater.* **2009**, *120*, 447–453.
- [53] Q. Liu, P. DeShong, M. R. Zachariah, *J. Nanopart. Res.* **2012**, *14*, 923–930.
- [54] I. Willner, E. Katz, *Angew. Chem., Int. Ed.* **2000**, *39*, 1181–1218.
- [55] Q. Zhang, R. F. Huang, L.-H. Guo, *Chin. Sci. Bull.* **2009**, *54*, 2620–2626.
- [56] V. Silin, H. Weetall, D. J. Vanderah, *J. Colloid Interface Sci.* **1997**, *185*, 94–103.
- [57] B. T. Houseman, M. Mrksich, *Chem. Biol.* **2002**, *9*, 443–454.
- [58] A. Wolcott, D. Gerion, M. Visconte, J. Sun, A. Schwartzberg, S. Chen, J. Z. Zhang, *J. Phys. Chem. B* **2006**, *110*, 5779–5789.
- [59] Y.-S. Cho, T.-J. Yoon, E.-S. Jang, K. Soo Hong, S. Young Lee, O. Ran Kim, C. Park, Y.-J. Kim, G.-C. Yi, K. Chang, *Cancer Lett.* **2010**, *299*, 63–71.
- [60] P. K. Smith, R. I. Krohn, G. T. Hermanson, A. K. Mallia, F. H. Gartner, M. D. Provenzano, E. K. Fujimoto, N. M. Goedeke, B. J. Olson, D. C. Klenk, *Anal. Biochem.* **1985**, *150*, 76–85.
- [61] K. J. Wiechelman, R. D. Braun, J. D. Fitzpatrick, *Anal. Biochem.* **1988**, *175*, 231–7.